Effective medium approximation for deeply subwavelength all-dielectric multilayers: when does it break down?

Lavrinenko, Andrei; Zhukovsky, Sergei; Andryieuski, Andrei; Takayama, Osamu; Shkondin, Evgeniy; Malureanu, Radu; Jensen, Flemming

Published in:
Proceedings of SPIE

Link to article, DOI:
10.1117/12.2229220

Publication date:
2016

Document Version
Peer reviewed version

Citation (APA):
Lavrinenko, A., Zhukovsky, S., Andryieuski, A., Takayama, O., Shkondin, E., Malureanu, R., & Jensen, F. (2016). Effective medium approximation for deeply subwavelength all-dielectric multilayers: when does it break down? In *Proceedings of SPIE* (Vol. 9883). SPIE - International Society for Optical Engineering. https://doi.org/10.1117/12.2229220

Effective medium approximation for deeply subwavelength all-dielectric multilayers: when does it break down?

Andrei V. Lavrinenko*[a], Sergei V. Zhukovsky[a], Andrei Andryieuski[a], Osamu Takayama[a], Evgeniy Shkondin[a,b], Radu Malureanu[a], Flemming Jensen[b]
[a]DTU Fotonik – Department of Photonics Engineering, Technical University of Denmark, Bld. 343, DK-2800, Kongens Lyngby, Denmark;
[b]DTU Danchip–National Center for Micro- and Nanofabrication, Technical University of Denmark, Ørsteds Plads 347, DK-2800, Kongens Lyngby, Denmark

ABSTRACT

We report on theoretical analysis and experimental validation of the applicability of the effective medium approximation to deeply subwavelength (period $\leqslant\lambda/30$) all-dielectric multilayer structures. Following the theoretical prediction of the anomalous breakdown of the effective medium approximation [H. H. Sheinfux et al., Phys. Rev. Lett. 113, 243901 (2014)] we thoroughly elaborate on regimes, when an actual multilayer stack exhibits significantly different properties compared to its homogenized model. Our findings are fully confirmed in the first direct experimental demonstration of the breakdown effect. Multilayer stacks are composed of alternating alumina and titania layers fabricated using atomic layer deposition. For light incident on such multilayers at angles near the total internal reflection, we observe pronounced differences in the reflectance spectra (up to 0.5) for structures with different layers ordering and different but still deeply subwavelength thicknesses. Such big reflectance difference values resulted from the special geometrical configuration with an additional resonator layer underneath the multilayers employed for the enhancement of the effect. Our results are important for the development of new homogenization approaches for metamaterials, high-precision multilayer ellipsometry methods and in a broad range of sensing applications.

Keywords: effective medium approximation, metamaterial, subwavelength multilayers, atomic layer deposition, homogenization.

INTRODUCTION

The backbone of the whole concept of metamaterials defined as artificial composite materials, where the elements ("meta-atoms") are much smaller than the wavelength[1], is traditionally associated with the effective parameters. Since the geometry and composition of the meta-atoms can theoretically be arbitrary, the effective medium parameters of metamaterials such as negative refractive index[1-3] or near-zero dielectric permittivity[4] can be very different from those of the naturally occurring materials.

Effective parameters can in many cases be introduced through homogenization. The applicability of the homogenization procedure to particular metamaterials has been a topical and ongoing discussion since the conception of the field, see, for example an extended report of Simovsky[5]. It has been found that there are intricate meta-atom geometries that do not readily lend themselves to homogenization[6]. Breaking of homogenization happens not only due to violating of pure geometrical subwavelength scaling, but also due to the origin of high-k waves possessing wavevectors much larger than those of light waves in relevant materials[7-11]. However, the possibility of using the effective medium theory with geometries as simple as a multilayer dielectric stack under the principal condition of homogenization applicability, namely that the layer thicknesses must be small compared with the wavelength of light that interacts with them, has hardly ever been questioned from the very introduction of the effective medium approximation (EMA)[12]. Hence, all-dielectric subwavelength multilayers, in which no waves with extremely large wave vectors are supported, have been expected to unconditionally obey the EMA[13].

* alav@fotonik.dtu.dk; Phone: +45 4525 6392; Fax: +45 4593 6581

Recently, the theoretical paper by Sheinfux et al.[14] showed that this commonly believed assumption may fail in certain regimes even for the deeply subwavelength layer thicknesses (smaller than 1/50 of the wavelength). Namely, when the angle of incidence is approaching the critical angle of the total internal reflection, the multilayer stack and its effective-medium counterpart exhibit significantly different transmission. Moreover, it was shown that the spectra become sensitive to variations of the layer thicknesses on the scale of one nanometer, i.e. hundreds times smaller than the wavelength. Meantime, if the refractive index of the medium behind the multilayer is carefully chosen, the transmission spectra become dependent on the choice of the outermost layer, which opens the whole sequence, i.e., ABAB…AB vs. BABA…BA, totally contrary to the effective medium theory results. Accordingly to Sheinfux et al.[14] such "anomalous" EMA breakdown happens because the optical properties of the multilayer arise from the interference effects between phases of Fresnel reflection and transmission coefficients in the frustrated total internal reflection regime rather than between phases accumulated during wave propagation in subwavelength layers. Certainly, the incidence should happen close to a near-critical angle to make this contribution significant. Physically, the EMA breaks down because the waves become evanescent in low-index layers, where they must experience the total internal reflection, but remain propagating in the high-index layers. Since the layers are deeply subwavelength, the light wave may still propagate through the multilayer via tunneling, whereas the EMA does not capture this physics and prohibits wave propagation.

Breaking the effective medium approximation in the case of subwavelength dielectric multilayer may lead to a serious twist in the rules of multilayers application in optics. The optics of plane stratified media – the study of light propagation in photonic multilayer structures – is the cornerstone subject within the broader field of electrodynamics of inhomogeneous media[15]. Multilayers are subject to several simple and illustrative approaches for their analysis[15-17]. Being a one-dimensional system, multilayers nevertheless play a central role in modeling of many fabricated structures, especially when various planar deposition methods are involved[18]. For such practical purposes, photonic multilayers are one of the most extensively studied optical systems to date, with profound theoretical knowledge and many established

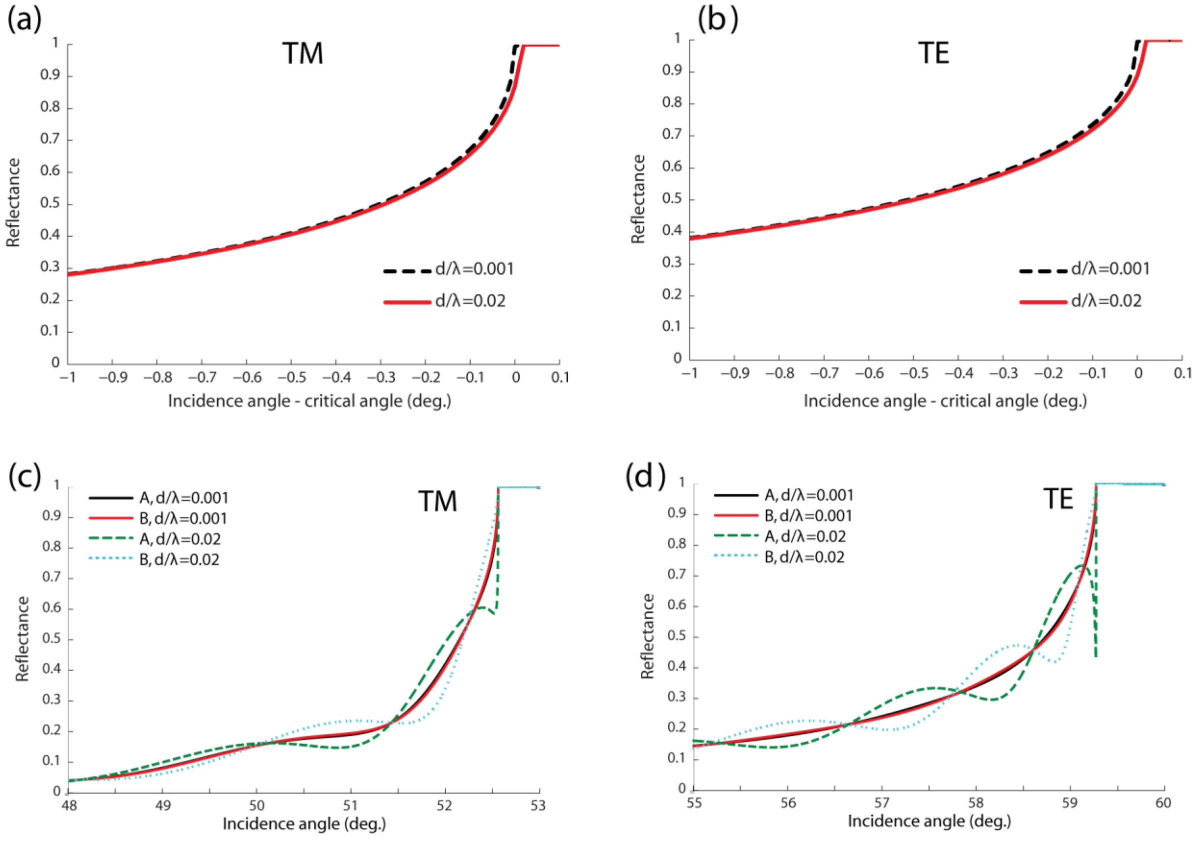

Figure 1. Reflectance difference between the actual periodic (d/λ=0.02) and quasi-homogenous (d/λ=0.001) structures for TM (left) and TE (right) polarizations: (a,b) for a semi-infinite periodic multilayer stack; (c,d) for a finite periodic stack with alternating opening layers designated as A or B, $n_A=2.0$, $n_B=3.0$; incident medium n=3, substrate $n_{sub} = 2.382$ (TM) and $n_{sub} = 2.579$ (TE).

applications. As a few characteristic examples, one may mention antireflection coatings, all-dielectric Bragg mirrors and omnidirectional reflectors[16, 19, 20], band-pass filters[16, 21, 22], and devices with enhanced nonlinear optical effects[23, 24]. Moreover, the optical multilayer model can be transferred to other physical systems governed by similar equations, such as acoustic multilayers[15, 25] and multiple-quantum-well heterostructures[26]. Thus understanding of all potential peculiarities of multilayers structures can have a strong impact on a rather broad domain of physics, especially taking into account concerns with homogenization of deeply subwavelength dielectric structures.

MODELING

The layout used in Sheinfux et al.[14] is well-chosen for a theoretical illustration of the very idea of the EMA breakdown. Nevertheless, in that layout the effect only becomes noticeable, when the multilayer contains few hundreds layers of each type. The firm requirement is that all the layers should be of equal thickness due to the extreme sensitivity of the effect on the layer parameters. Such structures, having 100-200 layers with extremely low tolerances would be impractical for any experimental realization. Especially in the optical regime, where it implies thicknesses of 10nm and tolerances below 1 nm. To facilitate the experimental verification and practical applications of this newly observed EMA breakdown, it is necessary to reproduce this effect in practically realizable structures. An alternative design was proposed by Andryieuski et al.[27] after methodical analysis of performance of a 1D stack and its homogenized analogue.

The reflectance of the system in different configurations is shown in Fig.1. When the semi-infinite multilayer is considered, some weak but distinctive deviations in reflectance of stacks composed of different but still deeply subwavelength layers are observed at angles really close to the critical angle of total reflection (Fig.1, a,b). Moreover, a finite stack deposited on a substrate exposes more pronounced reflectance disturbance (Fig. 1, c,d).

The reflectance difference can be remarkably enhanced further by employment of a resonator layer between the multilayer and the substrate[28]. The results of such implementation are illustrated in Fig.2, where the effect of parameters sweeping (the thickness of the additional layer L and substrate refractive index n_{sub}) is presented.

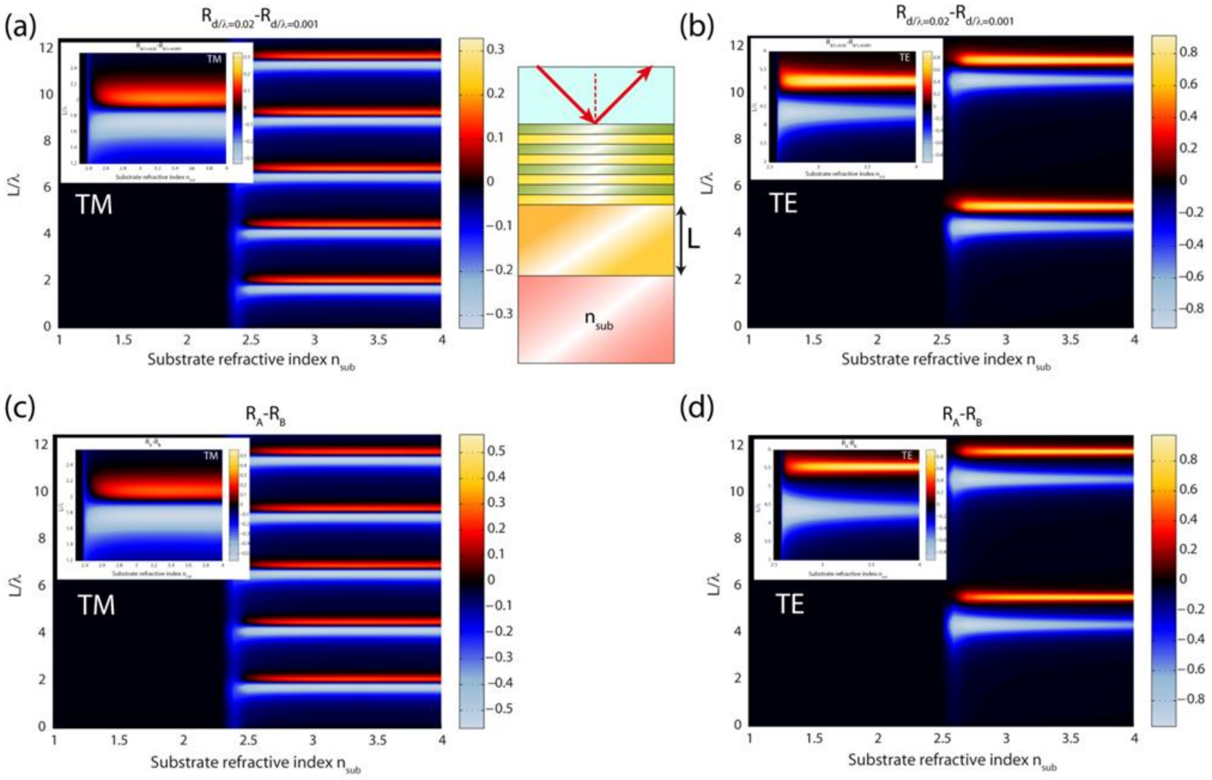

Figure 2. Reflectance difference between the actual periodic and quasi-homogenous structures for TM (a) and TE (b) polarizations for the finite stack with an additional resonator layer of refractive index n_{res} and thickness L. Reflectance difference for the periodic structure with starting layer A and B for TM (c) and TE (d) polarizations.

The primary factor affecting the enhancement of reflectance differences is the resonator thickness L; there are several maxima and minima experienced by the reflectance with changing L/λ. The dependence on substrate refractive index n_{sub} is much weaker and essentially consists in the requirement $n_{sub}>n_{res}$, where n_{res} states for the resonator layer refractive index. Resonator layer parameters can be separately optimized for TE and TM polarizations[27], e.g. $n_{res} = 2.382$ (TM) and $n_{res} = 2.579$ (TE). As it can be seen in Fig. 6 the EMA breakdown completely vanishes if $n_{sub} < n_{res}$. Once n_{sub} exceeds n_{res} substantially, any further variations of the substrate index have no effect on the observed differences.

FABRICATION AND CHARACTERIZATION

In order to check the conclusions and experimentally verify the EMA breakdown we fabricated four structures with configurations shown schematically in Fig.3 (Left part). Two of them comprise 20 alternating titania (high refractive index [H]) and alumina (low refractive index [L]) layers with d = 10 nm thickness and different layer ordering, [HL] or [LH] counting from the first layer after the Si_3N_4 resonator. Silicon nitride was chosen due to its index-matching properties $\varepsilon_{SiN} \approx (\varepsilon_H + \varepsilon_L)/2$ required for the resonator layer operation[27]. The other two samples comprise 10 alternating layers with double thickness d = 20 nm (so [HH] or [LL]), likewise with different layer ordering [HHLL] and [LLHH]. It is convenient to assign these designations for a supercell of the multilayers, thus the structures we have for characterization are $[HLHL]^5$, $[LHLH]^5$, $[HHLL]^5$, $[LLHH]^5$, where the superscript identifies the number of supercells in a particular sample.

The multilayers were fabricated with atomic layer deposition (ALD) using a hot-wall ALD system (Picosun R200). The precursors used for alumina and titania deposition were $Al(CH_3)_3$ / H_2O and $TiCl_4$ / H_2O respectively (both reagents coming from Sigma-Aldrich). The deposition temperature was 120°C. Full details of fabrication are given elsewhere[29]. All the deposited layers were of excellent quality with the total deviation of the multilayer thickness from the targeted 200 nm less than 1 nm (Fig. 4). After fabrication the refractive indices of titania (n_H) and alumina (n_L) were obtained by direct ellipsometry measurements.

The layout of the experimental arrangement is shown in Fig. 3 (Right). To observe the EMA breakdown effect experimentally, we employed a modified Otto-Kretchmann configuration. Since the incident angles of interest have to be close to the critical angle of total internal reflection, a high-index ambient medium is required. For this purpose we employed a semicylindrical prism made of zinc selenide ($n_{ZnSe} > n_H > n_L$). The multilayer sample was placed in close proximity to the semi-cylindrical ZnSe prism. The estimated angle of total internal reflection for our configuration θ is close to 52°. The light source was a super-continuum broadband laser (SuperK, NKT Photonics A/S, λ = 600 – 2500 nm). Its collimated output beam was polarized by a double Glan-Thompson polarizer and focused at the ZnSe-sample interface, using a set of off-axis parabolic mirrors. The reflected beam was collected to a multimode fiber using another parabolic mirror and led into an optical spectrum analyser (OSA, Yokogawa Electric Corp.) with the measuring range λ = 350 – 1750 nm. The working wavelengths range for the effect observation was λ = 610 – 1610 nm.

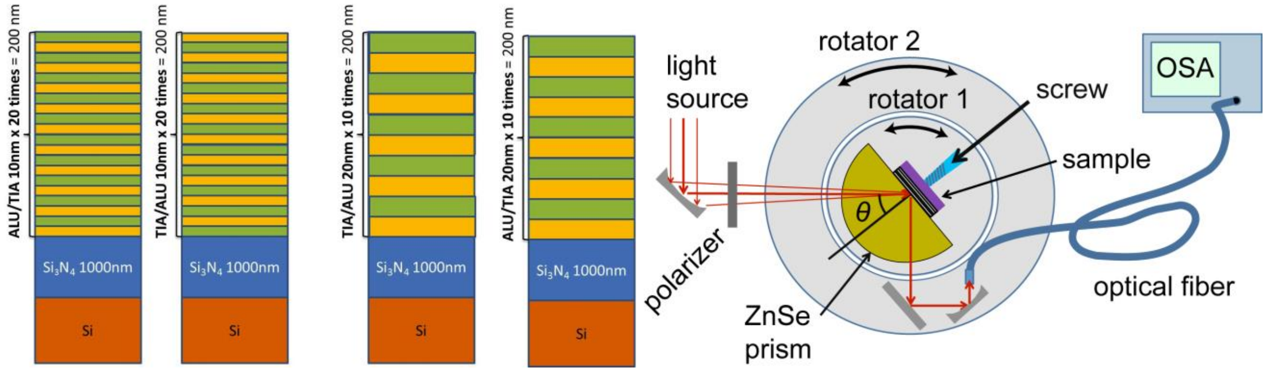

Figure 3. Left: Design of structures characterized for EMA breakdown. ALU states for an alumina layer, TIA – for titania. Right: Schematic illustration of set-up for experimental verification of the EMA breakdown.

The sample was attached to the prism with a custom-made holder tightened by a small-diameter screw. To minimize the air gap between the prism and the sample, which would have a dramatic influence on reflectance measurements according to the modelling results (especially for TM polarization), and to reduce the risk of dust trapping between the prism and the sample, the attachment of the sample was performed in the cleanroom. The quality of the attachment was monitored visually controlling the appearance of the Newton rings around the location of the screw on the holder as the screw was tightened.

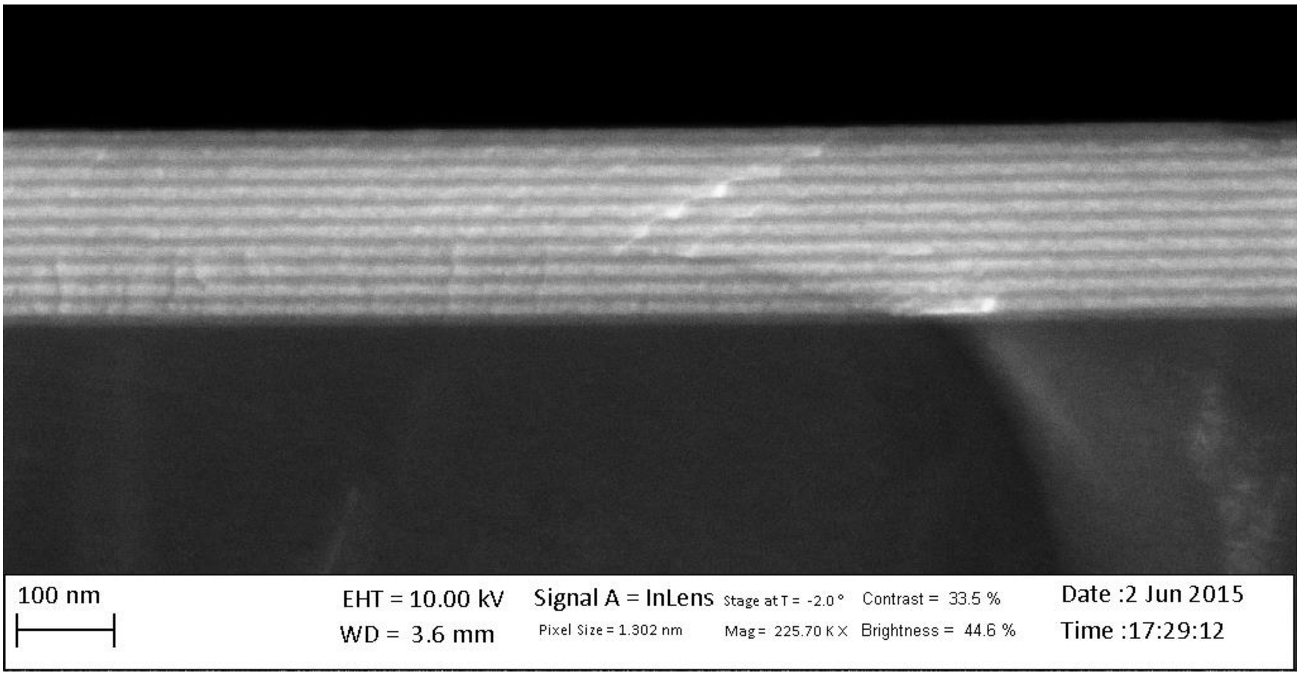

Figure 4. SEM image of the cross-section of one of ALD-deposited alumina/titania multilayer stacks with layer thickness 10 nm ($[HLHL]^5$).

Despite the preventive measures described above, the existence of an air gap between the prism and the sample could not be completely ruled out. In addition, the sharp dependence of the spectra on the incident angle (see Figs. 1-2) makes it necessary to control the incident angle with precision that might exceed the experimentally achievable one in the set-up used. To account for these two uncertainties, we have performed comparison between the theoretical and experimental results using two-parameter optimization. Specifically, we varied the air gap thickness and the systematic angle mismatch between the calculated and measured spectra, aiming at finding a global minimum in the total root mean square (RMS) error between theoretical and experimental reflectance spectra. The optimization maps are presented in Fig. 5a,b. It can be seen that the error is minimized for systematic angle mismatch of 0.2° and, quite surprisingly, zero gap thickness, confirming that an optical contact between the prism and the sample could be achieved without the use of any immersion fluid.

Both experimental and theoretical results for TE reflectance from the multilayers, obtained under the optimized conditions, are compared in Fig.5c for a range of θ between 20° and 54°. The corresponding reflectance difference, which is a signature of the EMA breakdown, is compared in Fig. 5d. We see that the reflectance exhibits small-amplitude ripples across the spectrum, in line with the theoretical expectation[29]. As θ approaches 52° the EMA breakdown becomes stronger, and difference in reflectance for different ordering of the layers reaches values around 0.4 – 0.5. Above 52° light undergoes total internal reflection ($R = 1$) for both samples. Overall, the measured reflectance behaves very close to the theoretical predictions. The only exception is at $\theta = 50°$, where the extreme sensitivity of the spectra to the incident angle in the vicinity of total reflection makes it immensely sensitive to all possible mismatch between theoretical and experimental parameters.

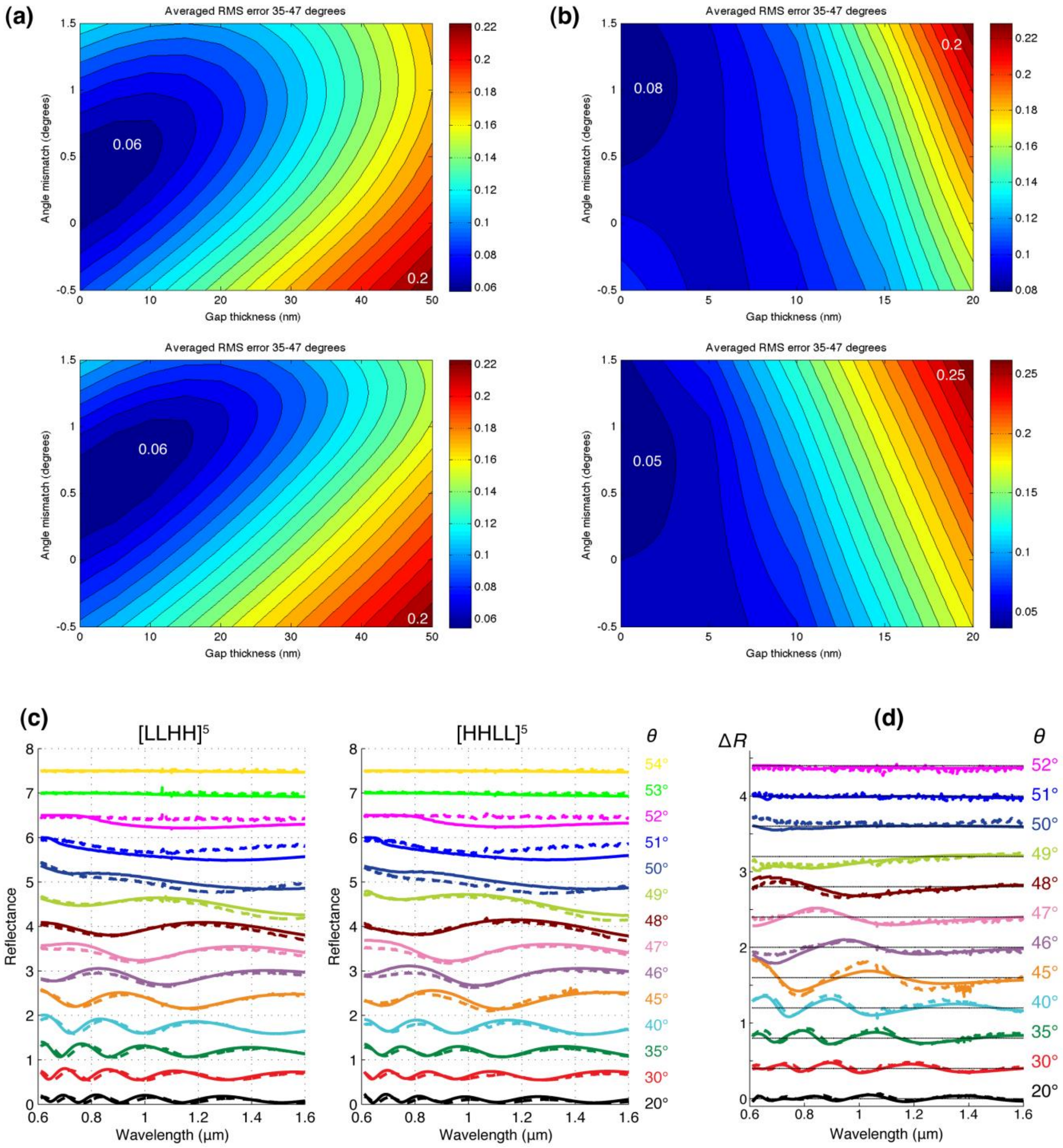

Figure 5. (a-b) Optimization maps showing the total RMS error between the theoretical and experimental spectra for (a) TE- and (b) TM-polarization for two samples: [LHLH]^5 (top) and [HLHL]^5 (bottom). (c-d) Direct comparison between theoretical (solid lines) and experimental (dashed lines) (c) individual reflectance spectra for two samples ([LLHH]^5 and [HHLL]^5) and (d) reflectance difference between these two samples in the TE polarization and for several incident angles θ between 20° and 54° (marked right most). Optimized matching conditions (systematic angle mismatch $\Delta\theta = 0.2°$ and gap thickness of 0 nm) were chosen.

The corresponding spectra in the TM polarization have a less mismatch and in overall fewer characteristic spectral features than for the TE case. However, non-zero differences in reflection from all pairs of samples (HHLL versus LLHH or HLHL versus HHLL, etc.) are still apparent.

CONCLUSIONS

We have experimentally demonstrated the effect of the EMA breakdown for all-dielectric multilayers with deeply subwavelength layer thicknesses from λ /30 to λ /160 and the total thickness of 200 nm, also smaller than the wavelength. The EMA breakdown manifests as the difference in the reflectance spectra of structures with different layer thickness (20 nm vs.~10 nm) as well as different layer ordering as shown in Fig.3. The reflectance difference reaches values of around 0.5, and is in good agreement with theoretical predictions. Our results can be used in ellipsometry of multilayer structures, both to correct the existing ellipsometry models that rely on the EMA, and to devise new models specifically based on the measurement of the features related to the EMA breakdown. Sensitivity of the reflectance difference to the layer thicknesses, angle and output material refractive index make the all-dielectric multilayer also suitable for various sensing applications.

Partial support from the People Programme (Marie Curie Actions) of the EU 7th Framework Programme FP7-PEOPLE-2011-IIF under REA grant agreement No. 302009 (Project HyPHONE) and VILLUM FONDEN blokstipendium (41/300-123012) is gratefully acknowledged. A.A. acknowledges support from the Danish Council for Independent Research via the GraTer project (Contract No. 0602-02135B).

REFERENCES

[1] Cai, W. and Shalaev, V., [Optical Metamaterials], Springer New York, New York, (2010).

[2] Shelby, R. A., Smith, D. R., and Schultz, S, “Experimental verification of a negative index of refraction,” Science 292, 77–79 (2001).

[3] Zhang, S., Fan, W., Panoiu, N., Malloy, K., Osgood, R. and Brueck, S., “Experimental demonstration of near-infrared negative-index metamaterials,” Phys. Rev. Lett. 95, 137404 (2005).

[4] Maas, R., Parsons, J., Engheta, N., and Polman, A., “Experimental realization of an epsilon-near-zero metamaterial at visible wavelengths”, Nature Photonics 7, 907–912 (2013).

[5] Simovski, C. R., “On electromagnetic characterization and homogenization of nanostructured metamaterials”, J. Opt. 13, 013001 (2011).

[6] Andryieuski, A., Menzel, C., Rockstuhl, C., Malureanu, R., Lederer, F. and Lavrinenko, A., “Homogenization of resonant chiral metamaterials”, Phys. Rev. B 82, 235107 (2010).

[7] Avrutsky, I., Salakhutdinov, I., Elser, J., and Podolskiy, V., “Highly confined optical modes in nanoscale metal-dielectric multilayers”, Phys. Rev. B 75 241402 (2007).

[8] Kidwai O., Zhukovsky, S. V., and Sipe, J. E., “Dipole radiation near hyperbolic metamaterials: applicability of effective-medium approximation”, Opt. Lett. 36, 2530–2532 (2011)

[9] Kidwai, O., Zhukovsky, S. V., and Sipe, J. E., “Effective-medium approach to planar multilayer hyperbolic metamaterials: Strengths and limitations”, Phys. Rev. A 85, 053842 (2012).

[10] Zhukovsky, S. V., Kidwai, O., and Sipe, J. E., “Physical nature of volume plasmon polaritons in hyperbolic metamaterials”, Opt. Express 21, 14982–14987 (2013).

[11] Zhukovsky, S. V., Andryieuski, A., Sipe, J. E., and Lavrinenko, A. V., “From surface to volume plasmons in hyperbolic metamaterials: General existence conditions for bulk high-k waves in metal-dielectric and graphene-dielectric multilayers”, Phys. Rev. B 90, 155429 (2014).

[12] Rytov, S. M., “Electromagnetic properties of a finely stratified medium”, Sov. Physics JETP 2, 466–475 (1956).

[13] El-Haija, A. J. A., “Effective medium approximation for the effective optical constants of a bilayer and a multilayer structure based on the characteristic matrix technique”, J. Appl. Phys. 93, 2590–2594 (2003).

[14] Sheinfux, H. H., Kaminer, I., Plotnik, Y., Bartal, G., and Segev. M., “Subwavelength multilayer dielectrics: ultrasensitive transmission and breakdown of effective-medium theory”, Phys. Rev. Lett. 113, 243901 (2014).

[15] Brekhovskikh, L. M., [Waves in Layered Media], Academic Press, New York, (1980).

[16] Yeh, P., [Optical waves in layered media], Wiley, Hoboken, New Jersey, (2005).

[17] Born, M., and Wolf, E., [Principles of Optics], Cambridge University Press, Cambridge, (1999).

[18] Macleod, H. A., [Thin-Film Optical Filters], Taylor & Francis (2010).

[19] Winn, J., N., Fink, Y., Fan, S., and Joannopoulos, J. D. “Omnidirectional reflection from a one-dimensional photonic crystal”, Opt. Lett. 23, 1573-1575 (1998).

[20] Chigrin, D. N., Lavrinenko, A. V., Yarotsky, D. A., and Gaponenko, S. V., “Observation of total omnidirectional reflection from a one-dimensional dielectric lattice”, Appl. Phys. A 68, 25–28 (1999).

[21] Kozhukh, S., Zhukovsky, S., Yurkevich, I., Stepkova, S., Gaponenko, S., Lunevich, A., and Glukhov, Y., "Design of high-transmission multiband multilayer filters for Raman spectroscopy", J. Nanophotonics 6, 061704 (2012).

[22] Zhukovsky, S. V., Gaponenko, S. V., and Lavrinenko, A. V., "Optical filters based on fractal and aperiodic multilayers", in [Optics of Aperiodic Structures - Fundamentals and Device Applications] ed. L. Dal Negro Pan Stanford Publishing, Singapore, 91–142 (2014).

[23] D'Aguanno, G., Centini, M., Scalora, M., Sibilia, C., Bertolotti, M., Bloemer, M. J. and Bowden, C. M., 2002 "Generalized coupled-mode theory for $\chi^{(2)}$ interactions in finite multilayered structures", J. Opt. Soc. Am. B 19, 2111 (2002).

[24] Zhukovsky, S. V., and Smirnov, A. G., "All-optical diode action in asymmetric nonlinear photonic multilayers with perfect transmission resonances", Phys. Rev. A 83, 023818 (2011).

[25] Li, F., and Wang, Y., "Elastic wave propagation and localization in band gap materials: a review", Sci. China Physics, Mech. Astron. 55, 1734–1746 (2012).

[26] Zhukovsky, S. V., and Gaponenko, S. V., "Constraints on transmission, dispersion, and density of states in dielectric multilayers and stepwise potential barriers with an arbitrary layer arrangement", Phys. Rev. E 77, 046602 (2008).

[27] Andryieuski, A., Lavrinenko, A. V., and Zhukovsky, S. V., "Anomalous effective medium approximation breakdown in deeply subwavelength all-dielectric photonic multilayers", Nanotechnology 26, 184001 (2015).

[28] Markovich, D. L., Andryieuski, A., Zalkovskij, M., Malureanu, R. and Lavrinenko, A. V., "Metamaterial polarization converter analysis: limits of performance", Appl. Phys. B 112, 143–152 (2013).

[29] Zhukovsky, S. V., Andryieuski, A., Takayama, O., Shkondin, E., Malureanu, R., Jensen, F., and Lavrinenko, A. V., "Experimental demonstration of effective medium approximation breakdown in deeply subwavelength all-dielectric multilayers", Phys. Rev. Lett 115, 177402 (2015).